Journal of Materials Chemistry A

Accepted Manuscript

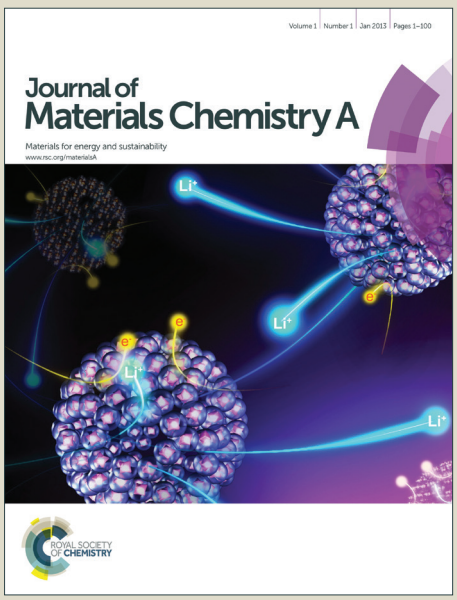

ROYAL SOCIETY OF CHEMISTRY

www.rsc.org/materialsA

Cite this: DOI: 10.1039/c0xx00000x

www.rsc.org/xxxxxx

ARTICLE TYPE

The efficient separation of surfactant stabilized oil/water emulsions with a flexible and superhydrophilic graphene/TiO_2 composite membrane

Peng Gao,[+a,b] Zhaoyang Liu,[+a] Darren Delai Sun*[a] and Wunjern Ng[a,b]

Received (in XXX, XXX) Xth XXXXXXXXX 20XX, Accepted Xth XXXXXXXXX 20XX

DOI: 10.1039/b000000x

It is a worldwide challenge to efficiently separate surfactant stabilized oil/water emulsions. The existing separation membranes suffer either from fouling or from the incapability. In this study, it is the first time to realize the efficient separation of surfactant stabilized oil/water emulsions *via* the delicate design and fabrication of a hierarchically nanostructured graphene/TiO_2 membrane. During the oil/water separation process, this membrane shows the combined advantages of high oil rejection rate and ultralow membrane fouling, thanks to its interconnected three-dimensional (3D) nanoscale network, underwater superoleophobic interface, and self-cleaning function. Furthermore, the mechanical flexibility of this membrane endows its great potential for wide industrial applications.

Introduction

The increasing oil/water mixtures discharged from frequent oil spill accidents, emerging shale oil fracking process and traditional petroleum industry are posing unprecedented threat on the already-vulnerable environmental system.[1-5] Especially in the presence of surfactants, these oil/water mixtures turns into small emulsion droplets of less than one micrometre, which are much stable and difficult to be separated, and remains a worldwide challenge. Conventional gravity separators and skimming techniques are incapable of separating emulsions.[6] Significant attentions have been paid to membrane technology in oil/water separation due to its high efficiency, small footprint, and easy scale-up.[7-11]

Typically, there are two kinds of membranes including hydrophobic and hydrophilic membranes, and both of them have been tried to separate oil/water mixture.[12] It should be noted that hydrophilic membranes are advantageous over hydrophobic membranes because: (1) they allow water to permeate, which prevents membrane clogging by viscous oil; (2) they avoid the formation of water barrier layer between the membranes and the oil phase, in contrast to the issue with hydrophobic and oleophilic membranes that water naturally settles below oil and form a barrier layer to prevents oil permeation.[8, 13-15] In this sense, ceramic porous membranes is a good choice for oil/water separation, due to their relatively hydrophilic property.[16] However, the poor mechanical flexibility and prohibitively high cost severely limit the wide applications of these ceramic membranes. Flexibility property is critically important for membrane applications, because the majority of current industrial applications adopt the spiral-wound type of membrane modules, in which the membranes can be rolled up and subsequently the required footprint can be significantly reduced. Therefore, it has been strongly desired to develop a novel membrane with both flexible and highly hydrophilic properties for effectively separating surfactant stabilized oil/water emulsions, with the features of high oil rejection rate and low membrane fouling.

As shown in previous studies, it is impracticable to adopt the well-established traditional phase inversion method, which has been widely used in porous hydrophobic membranes, for the fabrication of a porous hydrophilic membranes.[14] Therefore, people circumvented to fabricate porous hydrophilic membranes by coating hydrophilic materials on the surfaces of porous matrix (metal or polyester meshes). For example, Kota et al. coated hydro-responsive polymers on stainless steel meshes, and these superhydrophilic and superoleophobic membranes achieved 99.9% separation efficiency towards surfactant free oil/water emulsions, as well as free oil and water mixtures;[12] Jiang and co-workers coated polyacrylamide (PAM) hydrogel on stainless steel meshes, and these superhydrophilic and underwater superoleophobic membranes were used for the separation of crude oil/water mixture;[17] and very recently, Jin's group grew inorganic nanowires on copper mesh for effectively separating both immiscible oil/water mixtures and oil-in-water emulsions.[18] However, all these reported hydrophilic membranes are incapable of separating surfactant stabilized oil/water emulsions, mainly due to their intrinsic drawback of large pore sizes (usually more than one micrometre) in their selected porous matrix. In addition, another weakness caused by the large pore sizes in their membranes is that the low breakthrough value, which constrains their operations only under gravity rather than pressure.[12] It is well known that, compared with pressure-driven processes, gravity-driven processes for oil/water separation needs an additional time for de-emulsification, which subsequently results in low productivity in comparable time.[19] Therefore for practical oil/water separation, it makes more sense to fabricate a pressure-driven, instead of gravity-driven, hydrophilic membrane.

In this study, we are aiming to design and fabricate a pressure-

driven membrane with the features of high oil rejection rate and low membrane fouling for efficient separation of surfactant stabilized oil/water emulsions. This novel membrane is made of sulfonated grapheme oxide (SGO) nanosheets and hierarchically nanostructured TiO_2 spheres. The reason we chose these hierarchically nanostructured TiO_2 spheres as the building blocks of the membrane is because of their superhydrophilic interface and photocatalytic self-cleaning function, as shown in our previous studies.[20-22] Wherein, the nanoscale pore structure will ensure them with high oil rejection rate, and superhydrophilic interface and photocatalytic self-cleaning function will collectively ensure them with ultralow membrane fouling. However, these TiO_2 sphere membranes are short of mechanical flexibility. Recently, graphene nanosheets have emerged as promising nanomaterials in water purification and desalination devices, mainly owing to the advantageous features of mechanical flexibility.[23-25] In this study, SGO nanosheets with high hydrophilicity was chosen as the glue to chemically and physically bind the individual TiO_2 spheres together, endowing this composite membrane with excellent mechanical flexibility. For the first time, we demonstrated a flexible and superhydrophilic SGO-TiO_2 membrane is capable for the effective separation of surfactant stabilized oil/water emulsion.

Experimental

Materials

Sodium 2-chloroethanesulfonate hydrate ($ClCH_2CH_2SO_3H$), tetrabutyl titanate (TBT), sodium nitrate ($NaNO_3$, 99%), potassium permanganate ($KMnO_4$, 99%), hydrogen peroxide (H_2O_2, 35%), concentrated sulfuric acid (H_2SO_4, 98%), hydrochloric acid (HCl, 37%) and sodium hydroxide (NaOH) were obtained from Sigma-Aldrich. Dimethyl formamide (DMF) and isopropyl alcohol (IPA) were purchased from Merck Ltd. In addition, natural graphite (SP1) was obtained from Bay Carbon Company (USA). All chemicals were used without further purification. Furthermore, deionized (DI) water was produced from Millipore Milli-Q water purification system.

Fabrication of SGO-TiO_2 membrane

SGO nanosheets and TiO_2 nanospheres were synthesized according to the reported methods (See details in Supplementary methods).[26-28] SGO-TiO_2 composites were prepared by mixing 10 mg of as-synthesized SGO and 200 mg of as-prepared hierarchical TiO_2 sphere in DI water under ultrasonication. 100 mg of SGO-TiO_2 composites was dissolved into 100 mL of DI water to form a uniform suspension. The suspension was later injected into the filtration cup with one piece of commercial cellulose acetate (CA) membrane (Φ 47 mm, 0.45 μm, Millipore, USA) on the bottom of the cup. A layer of SGO-TiO_2 membrane was uniformly assembled on the surface of CA membrane after switching on the nitrogen gas for 30 min. The membrane was dried under 60°C overnight. The SGO-TiO_2 membrane was further compressed using a hot press under 5 bar at 100°C to enhance the connection and mechanical strength.

Characterization

The morphologies of SGO-TiO_2 and TiO_2 membrane were evaluated by field emission scanning electron microscopy (FESEM, JSM-7600F) and transmission electron microscopy (TEM, JEOL 2010-H). Surface topography and roughness of SGO-TiO_2 membrane were characterized by atomic force microscopy (AFM, PSIA XE-150). The crystal phase of SGO-TiO_2 was examined by X-ray diffraction (XRD, Shimadzu XRD-6000) with monochromated high-intensity Cu Kα radiation (λ=1.5418 Å) operated at 40 kV and 30 mA. Contact angles (CA) were measured on the VCA Optima machine (USA). The water droplets (3 μL) were dropped onto the surface of the membrane and the measurements were done at three different positions of each membrane. For underwater CA, the membrane was first immersed in water. A 5 μL dichloromethane (DCM) droplet was dropped carefully on the membrane and the CA was calculated based on the average value of three measurements. The droplet sizes of oil-in-water emulsions were measured by dynamic light scattering (DLS) by using Master sizer-2000. The water content in the permeate solution was measured using a Perkin Elmer Thermogravimetric Analyzer TGA 7 with Thermal Analysis Controller TAC 7/DX. The sample was heated from room temperature to 110 °C at a rate of 5 °C min^{-1} and kept at 110 °C for 30 min. The optical microscopy images of oil-in-water emulsions were taken on Olympus TH4-200 (Japan) by dropping an emulsion solution on one piece of glass slides.

Preparation of surfactant stabilized oil-in-water emulsions

Surfactant stabilized oil-in-water emulsions were prepared by mixing surfactant (Triton, X-100), water and oil (namely toluene, crude oil, vegetable oil and diesel) in a ratio of 2:100:1 v/v/v and sonicated under a power of 1kW for 1 h to produce a white and milky solution. The droplet sizes of toluene-in-water emulsion are around 200 nm measured by DLS. The surfactant stabilized oil-in-water emulsions were stable for several weeks and no de-emulsification was observed.

Oil/water separation

Oil/water separation performance of the membrane was investigated by a vacuum filtration setup, as shown in Fig. 3b. The surfactant stabilized oil-in-water emulsions were poured into the filtration cup. When the vacuum pump was turned on, the water permeated through the membrane into the container, while the oil droplets were rejected on the membrane surface.

Self-cleaning experiment

The SGO-TiO_2 membrane was contaminated with oleic acid by immersing the membrane into a acetone solution of oleic acid (5wt%) for 10 min. The contaminated membrane was put under UV irradiation for 10 min after each cycle. The water CA of the contaminated membrane before and after UV irradiation was also measured.

Results and discussion

Surface morphology and microstructure of as-synthesized membranes

The XRD pattern of as-synthesized SGO-TiO_2 membrane indicates that the crystal phase of TiO_2 is anatase except a trace amount of brookite (marked by asterisk), as shown in Fig. S1. Fig. 1a shows that the mechanical strength of pure TiO_2 nanosphere membrane is vulnerable. The pure TiO_2 membrane is

broken

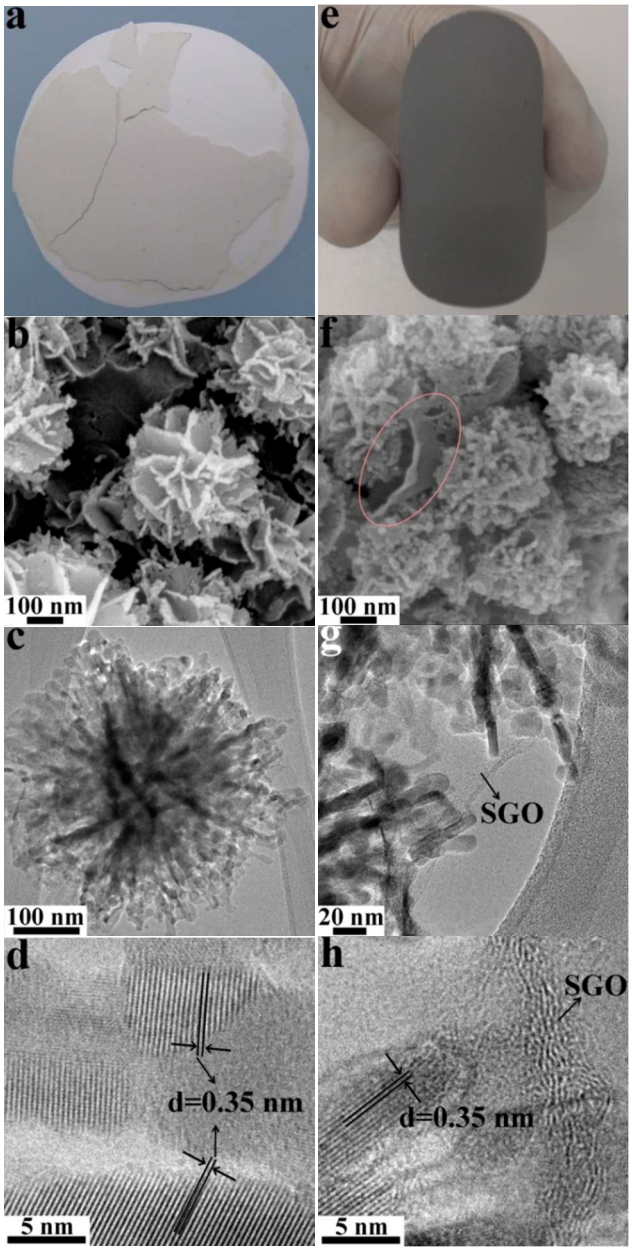

Fig. 1 (a) Digital photo of the pure TiO_2 nanosphere membrane, showing the membrane breaks into several pieces after bending; (b) FESEM image of surface morphology of the pure TiO_2 nanosphere membrane; (c) TEM image of a single TiO_2 nanosphere; (d) HRTEM image of the TiO_2 nanosphere; (e) Digital photo of the novel SGO-TiO_2 membrane, showing its good flexibility; (f) FESEM image of surface morphology of the novel SGO-TiO_2 membrane; (g) TEM image of SGO-TiO_2 composites showing SGO sheets link two TiO_2 nanospheres together; and (h) HRTEM image of SGO-TiO_2 composites.

easily when it is bended with hands. The surface morphology of the pure TiO_2 nanosphere membrane indicates that the TiO_2 nanospheres are packed together loosely with the pore size larger than 100 nm, as shown in Fig. 1b. Lack of cross-linkage between the TiO_2 nanospheres results in the poor mechanical strength and big pore size. Fig. 1c shows the TEM image of a single TiO_2 nanosphere with a diameter of about 380 nm. The TiO_2 nanosphere is in fact constructed by thin nanosheets which are assembled by nanoparticles. Fig. 1d is the HRTEM image of a TiO_2 nanosphere and the distinct lattice fringe of 0.35 nm can be assigned to the (101) crystal plane of anatase TiO_2. Graphene oxide (GO) has been reported as the good cross-linker for the inorganic materials due to the existence of a large amount of hydrophilic functional groups.[29-31] In this work, sulfonated graphene oxide (SGO) was chosen as the cross-linker to bond TiO_2 nanospheres together with an efficient cross-linking method. It is interesting to note that the SGO-TiO_2 membrane is mechanically flexible and can be freely bended due to the cross-linking effects of SGO sheets, as shown in the inset of Fig. 1e. This excellent flexibility can broaden the practical applications of this novel membrane by fitting in various configurations of membrane modules. Fig. 1f is the FESEM surface morphology of the novel SGO-TiO_2 membrane. The TiO_2 nanospheres are bound together by SGO sheets (as marked by red ellipse), leading to a much denser membrane compared with pure TiO_2 nanosphere membrane in Fig. 1b. Fig. 1f indicates that the pore sizes of the novel SGO-TiO_2 membrane are less than 100 nm, which is critically important for the separation of oil-in-water emulsions with small droplets. The pore size of the SGO-TiO_2 membrane was further determined by filtering different molecular weights of dextran solution, as shown in Fig. S2, which exhibited the pore size was around 60 nm. In order to thoroughly investigate the microstructure of the SGO-TiO_2 membrane, one small piece of the membrane was ultrasonically dispersed in ethanol and put under TEM characterization. Fig. 1g is the TEM image of SGO-TiO_2 composites. SGO sheets can be clearly indentified under TEM due to their special two-dimensional and thin morphology, as marked by dark arrows. SGO sheets act like "bridges" to connect two TiO_2 nanospheres together. The characteristic wrinkles of SGO sheets and clear lattice fringe of anatase TiO_2 can be unambiguously observed in the HRTEM image of SGO-TiO_2 composites, as shown in Fig. 1h.

Surface roughness and wetting behavior

Generally, the wettability of a membrane depends on both the chemical composition and the geometrical structure (surface roughness).[16, 32, 33] A high surface roughness enhances the hydrophilic property of the solid surface according to the equation: $\cos\theta_a = r\cos\theta$ (θ_a is the apparent water contact angle (CA) on a rough surface, θ is the CA on a smooth surface and r is the surface roughness factor).[32, 34] The 2D AFM images in Fig. 2a shows that the SGO-TiO_2 membrane surface is very dense without observable gaps. In addition, the 3D AFM image shows that the SGO-TiO_2 membrane surface is quite rough with about 250 nm undulation range, as shown in Fig. 2b. The high roughness can enhance the hydrophilic property.[17] Fig. 2c and d show the water CA and underwater oil CA of this membrane, respectively. A nearly zero (0°) water CA and ~152° underwater oil CA are obtained, demonstrating the surface of this SGO-TiO_2 membrane is superhydrophilic and underwater superoleophobic. A high-speed camera system was used to record the spreading process of a water droplet to investigate the wetting behavior of water on the SGO-TiO_2 membrane, as shown in Fig. 2e. A water droplet (3 μL) spreads out very quickly when it contacts the membrane surface, and the whole process is completed less than 0.1 s, indicating a superior property of this membrane for water

wetting. These specific surface properties are favorable for water permeation, while rejecting oil.

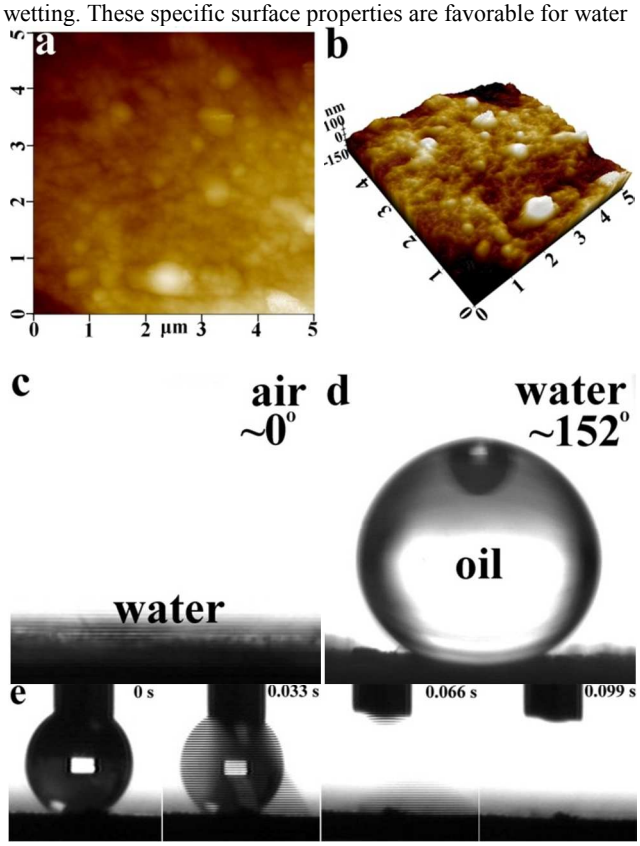

Fig. 2 (a) Two dimensional (2D) and (b) three dimensional (3D) AFM images of SGO-TiO_2 membrane, respectively; (c) Photograph of a water droplet on the membrane surface showing nearly zero contact angle; (d) Photograph of an underwater oil droplet (DCM) on the membrane surface showing contact angle of ~152°; and (e) Wetting values as a function of deposited time showing a water droplet spreading quickly on the membrane within 0.099 s.

Separation of surfactant stabilized oil-in-water emulsions

The oil/water separation performance of the novel SGO-TiO_2 membrane was investigated by separating several kinds of surfactant stabilized oil-in-water emulsions with droplet sizes in the nanometer and micrometer scales, including toluene-in-water, crude oil-in-water, and vegetable oil-in-water. The separation mechanism was schematically illustrated in Fig. 3a, wherein, water can easily permeate through this novel membrane, while oil droplets are rejected due to the underwater superoleophobic interface and nanoscale pore size. Fig. 3b shows the process for the separation of toluene-in-water emulsion. Initially, toluene-in-water emulsion was put in the filtration cup of the filtration system. The water (the red color is originated from Rhodamine B indicator) permeated through the membrane quickly when the vacuum pump was turned on, while toluene was repelled by the membrane, due to the superhydrophilic and underwater superoleophobic properties of this membrane. The separation efficiencies of this novel membrane with different oil-in-water emulsions are shown in Fig. 3c. Remarkably, this membrane exhibits extremely high separation efficiency (> 99.9%) with all investigated surfactant stabilized oil-in-water emulsions, including 99.92% for toluene-in-water, 99.94% for crude oil-in-water, and 99.91% for vegetable oil-in-water. In addition, optical microscopy was adopted to observe the droplets in the feed of toluene-in-water emulsion and the permeate to further confirm the high separation efficiency of this novel SGO-TiO_2 membrane towards surfactant stabilized oil-in-water emulsions. Typically, the surfactant (Triton) plays a vital role in the oil-in-water emulsions. The size of oil droplets is in the range of 1 to 50

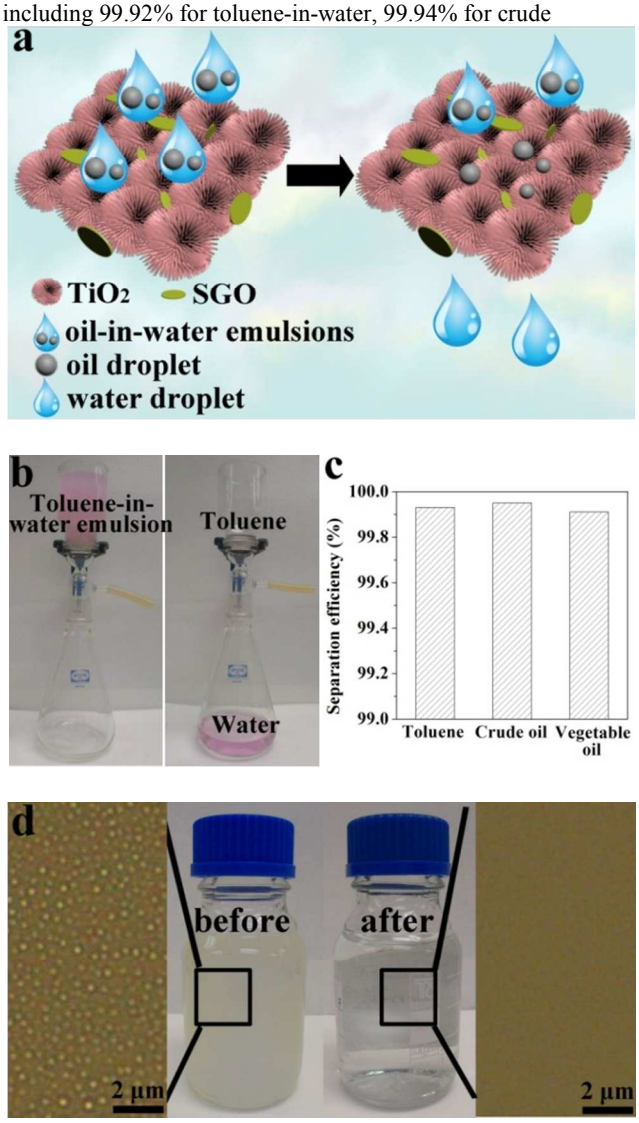

Fig. 3 (a) The schematic illustration of the structure of the novel SGO-TiO_2 membrane and the process of oil/water separation. It shows water can permeate through the membrane while oil cannot; (b) Digital photos: (left) before separation of toluene-in-water emulsions and (right) after separation of toluene-in-water emulsions with the novel SGO-TiO_2 membrane; (c) separation efficiencies of different oil-in-water emulsions; and (d) Optical microscopy images of toluene-in-water emulsions before and after oil/water separation with the novel SGO-TiO_2 membrane. Left side is the optical microscopy image of toluene-in-water emulsions before separation showing the size of oil droplets is around 200 nm; middle is digital photos of toluene-in-water emulsions before and after oil/water separation; right side is the optical microscopy image of toluene-in-water emulsions after oil/water separation showing no oil droplets can be observed.

μm without surfactant (see Supplementary Fig. S3). However, the size of oil droplets was significantly reduced when the surfactant was added, and the average droplet size is about 200 nm, as shown in the left side of Fig. 3d. The droplet size distribution was confirmed by dynamic light scattering (DLS) measurements (see Supplementary Fig. S4). After the separation process, no droplets are observed in the collected permeate (right side of Fig. 3d), confirming this SGO-TiO_2 membrane is highly efficient to separate the surfactant stabilized oil-in-water emulsions with oil droplet sizes less than 1 μm.

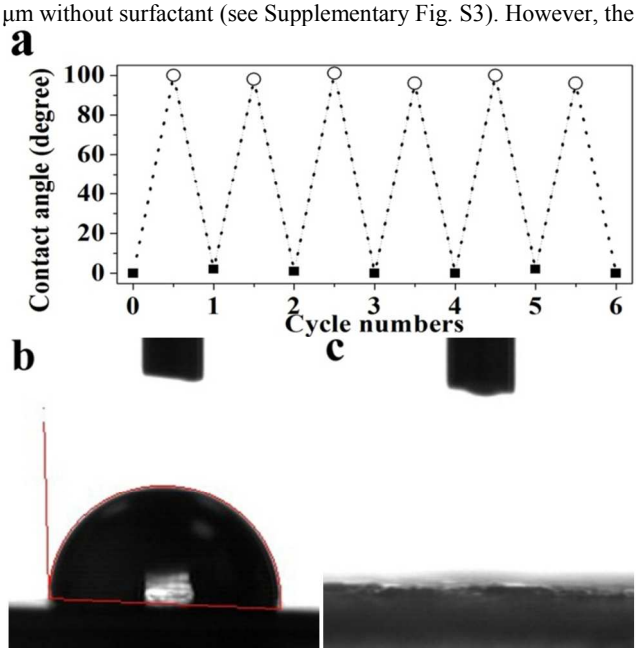

Fig. 4 (a) Changes of water CA before and after UV irradiation during 6 cycles; (b) Photograph of a water droplet on the membrane surface showing a water CA of ~100° because of oleic acid contamination before UV irradiation; and (c) Photograph of a water droplet on the membrane surface showing a water CA of ~0° after UV irradiation, indicating the membrane can restore its superhydrophilicity.

Self-cleaning property

Membrane fouling significantly restricts the application of membrane in oil/water separation and water purification fields. In the presence of water soluable or unsoluable organic matters, they tend to deposit on the surface of membrane, which greatly reduces the water flux.[35] TiO_2 is a well-known photocatalytic material which can generate strong reactive species, including hydroxyl radicals and superoxide anions, under UV irradiation.[36, 37] In addition, the photocatalytic activity can be enhanced due to the presence of SGO sheets which can facilitate the charge separation rate. Therortically, the membrane fouling of this novel SGO-TiO_2 membrane can be eliminated because the organic matters can be decomposed by the reactive sepecies. In this work, the capability of this novel SGO-TiO_2 membrane for separation of contaminant contained oil-in-water emulsions was investigated by immersing the membrane into the oleic acid/acetone solution. Fig. 4a shows the changes of CA before and after UV irradiation within 6 cycles. After oil/water separation, the superhydrophilic property of the membrane was destroyed because the membrane was contaminated by oleic acid. The membrane showed a hydrophobic property with a water contact angle of ~100°, as shown in Fig. 4b. After UV irradiation, the membrane could totally restore its superhydrophilicity, with a water contact angle of ~0°, as shown in Fig. 4c. This is because this novel membrane acquires prominent photocatalytic activity and high photodegradation efficiency towards organic pollutants, which significantly alleviates the membrane fouling. In addition, this membrane can remain the relative high flux of 84 L/m^2·h during the oil/water separation process, and the flux can be recovered to the initial state after a simple membrane washing, as shown in Fig. S5. These results indicate that this novel membrane can be applied in practical oil/water separation process.

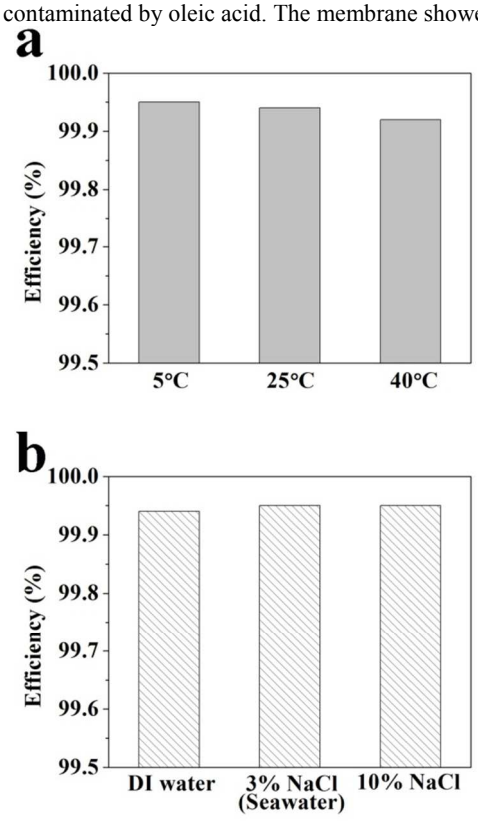

Fig. 5 (a) Separation efficiency of crude oil-in-water emulsions at different temperature; and (b) Separation efficiency of crude oil-in-water emulsions at different ionic concentration.

Practical oil/water separation

To investigate the practical oil/water separation ability, this novel SGO-TiO_2 membrane was adopted to separate the crude oil-in-water emulsions at different temperature and ionic concentration. Fig. 5a shows that the separation efficiency of this novel membrane slightly decreases with increasing the temperatures of the crude oil/water mixture, which is attributed to that the solubility of oil in water is higher at higher temperatures.[38] The separation efficiency at 40 °C is slightly decreased from 99.94% to 99.91%, indicating the applicability of this membrane in a wide temperature range. Different concentrations of NaCl solutions were mixed with crude oil to investigate the effects of ionic concentrations on the separation efficiency of this membrane. Fig. 5b shows that the concentration of NaCl has almost no influence on the separation efficiency, and the overall

separation efficiency can reach as high as 99.94%. The above results demonstrate that this novel SGO-TiO_2 membrane can be applied in industrial oily wastewater treatment and marine oil spill cleanup.

Conclusions

In summary, a mechanically flexible, superhydrophilic, underwater superoleophobic and self-cleaning SGO-TiO_2 membrane was successfully fabricated for the first time. We demonstrated that this novel membrane had the ability for separating surfactant stabilized oil/water emulsions with high separation efficiency in terms of oil rejection rate. More importantly, the membrane presents an excellent anti-oil fouling and self-cleaning property for long term operation. Therefore, this novel membrane is promising for numerous applications, such as for treating oily wastewater from petroleum industry, bilge water and oil spills, especially those stabilized by surfactants.

Acknowledgements

Authors would like to acknowledge the Clean Energy Research Programme under National Research Foundation of Singapore for their research grant (Grant No. NRF2007EWT-CERP01-0420) support for this work. We appreciate Miss Anran Li for the helpful discussion.

Notes and references

[a] *School of Civil and Environmental Engineering, Nanyang Technological University, Singapore 639798. Email: DDSUN@ntu.edu.sg; Fax: +65 6791-0676; Tel: +65 6790-6273*
[b] *Nanyang Environment & Water Research Institute, Nanyang Technological University, Singapore 639798.*
[+] These authors contributed equally to this work.
† Electronic Supplementary Information (ESI) available: [Experimental details and XRD, DLS graphs]. See DOI: 10.1039/b000000x/

1. A. Asatekin and A. M. Mayes, *Environ. Sci. Technol.*, 2009, **43**, 4487-4492.
2. E. Kintisch, *Science*, 2010, **329**, 735-736.
3. K. Li, J. Ju, Z. Xue, J. Ma, L. Feng, S. Gao and L. Jiang, *Nat. Commun.*, 2013, **4**, 2276-2282.
4. M. Cheng, Y. Gao, X. Guo, Z. Shi, J.-f. Chen and F. Shi, *Langmuir*, 2011, **27**, 7371-7375.
5. G. Hayase, K. Kanamori, M. Fukuchi, H. Kaji and K. Nakanishi, *Angew. Chem. Int. Ed.*, 2013, **52**, 1986-1989.
6. M. Cheryan and N. Rajagopalan, *J. Membr. Sci.*, 1998, **151**, 13-28.
7. J. Yuan, X. Liu, O. Akbulut, J. Hu, S. L. Suib, J. Kong and F. Stellacci, *Nat. nanotechnol.*, 2008, **3**, 332-336.
8. C. Gao, Z. Sun, K. Li, Y. Chen, Y. Cao, S. Zhang and L. Feng, *Energy Environ. Sci.*, 2013, **6**, 1147-1151.
9. S. Maphutha, K. Moothi, M. Meyyappan and S. E. Iyuke, *Sci. Rep.*, 2013, **3**, 1509-1515.
10. L. Zhang, Z. Zhang and P. Wang, *NPG Asia Materials*, 2012, **4**, 1-8.
11. G. Kwon, A. K. Kota, Y. Li, A. Sohani, J. M. Mabry and A. Tuteja, *Adv. Mater.*, 2012, **24**, 3666-3671.
12. A. K. Kota, G. Kwon, W. Choi, J. M. Mabry and A. Tuteja, *Nat. Commun.*, 2012, **3**, 1025-1032.
13. L. Zhang, Y. Zhong, D. Cha and P. Wang, *Sci. Rep.*, 2013, **3**.
14. W. Zhang, Z. Shi, F. Zhang, X. Liu, J. Jin and L. Jiang, *Adv. Mater.*, 2013, **25**, 2071-2076.
15. Z. Shi, W. Zhang, F. Zhang, X. Liu, D. Wang, J. Jin and L. Jiang, *Adv. Mater.*, 2013, **25**, 2422-2427.
16. Q. Wen, J. Di, L. Jiang, J. Yu and R. Xu, *Chem. Sci.*, 2013, **4**, 591-595.
17. Z. Xue, S. Wang, L. Lin, L. Chen, M. Liu, L. Feng and L. Jiang, *Adv. Mater.*, 2011, **23**, 4270-4273.
18. F. Zhang, W. B. Zhang, Z. Shi, D. Wang, J. Jin and L. Jiang, *Adv. Mater.*, 2013, **25**, 4192-4198.
19. U. Daiminger, W. Nitsch, P. Plucinski and S. Hoffmann, *J. Membr. Sci.*, 1995, **99**, 197-203.
20. J. H. Pan, X. Zhang, A. J. Du, D. D. Sun and J. O. Leckie, *J. Am. Chem. Soc.*, 2008, **130**, 11256-11257.
21. X. Zhang, T. Zhang, J. Ng and D. D. Sun, *Adv. Funct. Mater.*, 2009, **19**, 3731-3736.
22. H. Bai, Z. Liu and D. D. Sun, *Chem. Commun.*, 2010, **46**, 6542-6544.
23. R. R. Nair, H. A. Wu, P. N. Jayaram, I. V. Grigorieva and A. K. Geim, *Science*, 2012, **335**, 442-444.
24. D. Cohen-Tanugi and J. C. Grossman, *Nano Lett.*, 2012, **12**, 3602-3608.
25. Y. Han, Z. Xu and C. Gao, *Adv. Funct. Mater.*, 2013, **23**, 3693-3700.
26. P. Gao, Z. Liu and D. D. Sun, *J. Mater. Chem. A*, 2013, **1**, 14262-14269.
27. H. B. Wu, X. W. Lou and H. H. Hng, *Chem. Eur. J.*, 2012, **18**, 2094-2099.
28. P. Gao, K. Ng and D. D. Sun, *J. Hazard. Mater.*, 2013, **262**, 826-835.
29. L. Zhu, L. Gu, Y. Zhou, S. Cao and X. Cao, *J. Mater. Chem.*, 2011, **21**, 12503-12510.
30. P. Gao, Z. Liu, M. Tai, D. D. Sun and W. Ng, *Appl. Catal. B: Environ.*, 2013, **138-139**, 17-25.
31. P. Gao, J. Liu, S. Lee, T. Zhang and D. D. Sun, *J. Mater. Chem.*, 2012, **22**, 2292-2298.
32. L. Kou and C. Gao, *Nanoscale*, 2011, **3**, 519-528.
33. X. Liu, J. Zhou, Z. Xue, J. Gao, J. Meng, S. Wang and L. Jiang, *Adv. Mater.*, 2012, **24**, 3401-3405.
34. X. Liu and J. He, *J. Phys. Chem. C*, 2008, **113**, 148-152.
35. P. Gao, M. H. Tai and D. D. Sun, *ChemPlusChem*, 2013, **78**, 1475-1482.
36. P. Gao, D. D. Sun and W. J. Ng, *RSC Adv.*, 2013, **3**, 15202-15210.
37. P. Gao, J. Liu, T. Zhang, D. D. Sun and W. Ng, *J. Hazard. Mater.*, 2012, **229–230**, 209-216.
38. Y. S. Wan, M. Bobra, A. M. Bobra, A. Maijanen, L. Suntio and D. Mackay, *Oil and Chemical Pollution*, 1990, **7**, 57-84.